

# Use Of Cu-C-TiO<sub>2</sub> In Dye Sensitized Solar Cell

Monika Trivedi, ChetnaAmeta, Meenakshi S. Solanki, RakshitAmetaand Surbhi Benjamin

**Abstract:** A novel and simple strategy has been used for the preparation of TiO<sub>2</sub> nanoparticles co-doped with carbon (non-metal) and copper (transition metal) by sol-gel method. The dye sensitized solar cell was fabricated with Cu-C-TiO<sub>2</sub> nanocrystalline layer on FTO conductive glass, sensitized with rhodamine B dye. I<sup>-</sup>/I<sub>3</sub><sup>-</sup> redox couple was used as liquid electrolyte and carbon (graphite) as counter electrode. The experimental results of rhodamine B sensitized Cu-C-doped TiO<sub>2</sub> showed V<sub>oc</sub>= 101.2 mV, i<sub>sc</sub>= 0.0545 mA, V<sub>pp</sub>= 55.9 mV and i<sub>pp</sub>= 0.0496 mA and FF = 0.50. The photo-to-electric power conversion efficiency was 0.004% under 66.0 mWcm<sup>-2</sup> light intensity. The undoped and Cu-C-TiO<sub>2</sub> nanoparticles were analyzed by X-ray diffraction (XRD), scanning electron microscopy(SEM) and Fourier transform infrared (FT-IR) techniques.

**Index Terms:** DSSC; Co-doped; FTO; Titanium dioxide; Solar cell; Copper sulfate; Rhodamine B; Carbon

## 1 INTRODUCTION

Solar energy is a promising and abundant source of energy to fulfil the future demands of world. Solar energy is being harvested all over the globe mainly using photovoltaic devices. Solar cells generate power by direct conversion of light into electricity by using semiconductor. The silicon panels are widely used for this purpose, but these are very costly and have complex technologies. The photovoltaic technology of polycrystalline thin-film based on silicon solar cells are the best option for sustainable future energy technology. The efficiencies of silicon and GaAs monocrystalline solar cells reached quite close to predicted theoretical values. The thin film solar cells based on CdTe and Cu(In,Ga)Se<sub>2</sub> were demonstrated to have record efficiencies [1]. Dye sensitized solar cell is thin film solar cell and it was invented by Gratzel and O'Regan [2]. However, it had been a very crucial issue to enhance its power conversion efficiency as compared to other solar devices. Hagfeldt [3] reported 12% power conversion efficiency by using molecular- and nanometer-scale components in the fabrication of DSSC. Nowadays, DSSC earned widespread attention because of their low cost manufacturing, approachable fabrication and modulated optical properties like variation in color and transparency Mathew et al. [4] used donor- $\pi$ -bridge-acceptor porphyrin dye SM315 for the sensitization of the solar cell, with cobalt (II/III) redox shuttle electrolyte. This cell shows about 13% power conversion efficiency. Different approaches have been attempted to achieve effective power conversion efficiency such as coating of insulating layer or higher band gap materials [5, 6]. Doping of TiO<sub>2</sub> with other elements is one of the efficient ways to modify its physical and chemical properties [7]. Doping of a semiconductor with metals and

non-metals shows improvement in the activity of that material. Doped semiconductor shows strong red shift of their absorption into the visible region as compared with undoped semiconductors [8]. Metal doping improved the open-circuit voltage due to the upward shift of the Fermi level while defect oxygen generated retardation in the negative shift of the Fermi level [9]. Doping with metals and non-metals such as nitrogen doped nanostructured titania electrode shows 8% power conversion efficiency [10]. 7.05% Efficiency was achieved with co-doped Tm<sup>3+</sup> and Yb<sup>3+</sup> TiO<sub>2</sub> sensitized with N719 dye for DSSC [11]. Indium doped ZnO (In-ZnO) compact layer and a TiO<sub>2</sub> protective layer has been developed by Zheng et al. [12]. This cell is 36% more efficient than unmodified In-ZnO DSSC. In the present work Cu-C-TiO<sub>2</sub> was synthesized by sol-gel method. The DSSC was fabricated with this co-doped TiO<sub>2</sub> and the effect of different parameters like dye concentration, electrolyte concentration, light intensity and exposed surface area of semiconductor on the electrical output was examined.

## 2. EXPERIMENTAL

### 2.1 Preparation of nanocrystalline pure and Cu-C-TiO<sub>2</sub>

Both pure and Co-doped Cu -C-TiO<sub>2</sub> were synthesized by using sol-gel method. 2 mL of titanium tetraisopropoxide was mixed with 10 mL of 2-propanol in a beaker. A solution of 10 g of CuSO<sub>4</sub> and 10 g fructose was prepared in 100 mL distilled water. Both these solutions were mixed with continuous stirring by a glass rod. Precipitates of Cu-C-Ti(OH)<sub>4</sub> was obtained. This mixture was transferred to the oven for drying at 60-110°C up to dryness. After cooling down to room temperature, it was calcined in furnace at 400°C for 3 hours. Again it was brought to room temperature and the obtained powder of Cu-C-TiO<sub>2</sub> was grinded in agate mortar with pestle to form fine crystals. The same procedure was followed to prepare undoped TiO<sub>2</sub> with the difference that no dopant was added (copper sulphate and fructose). It is schematically presented in Fig. 1.

- *Monika Trivedi, Department of chemistry, PAHER University, Udaipur-313003 (Raj) India,+91-8854030134, E-mail: monachem.01@gmail.com*
- *ChetnaAmeta, Department of chemistry, PAHER University, Udaipur-313003 (Raj) India,+91-7742795080, E-mail: Chetna.ameta789@gmail.com*
- *Meenakshi S. Solanki, Department of chemistry, PAHER University,Udaipur-313003 (Raj) India,+91-8502056533, E-mail: meenakshisingh001989@gmail.com*
- *Dr. RakshitAmeta, Department of chemistry, PAHER university, Udaipur-313003 (Raj) India, +91-9461179656, E-mail: rakshit\_ameta@yahoo.in*
- *Dr. Surabhi Benjamin, Department of chemistry, PAHER University, Udaipur-313003 (Raj) India, +91-9799297932, E-mail: surbhi.singh1@yahoo.com*

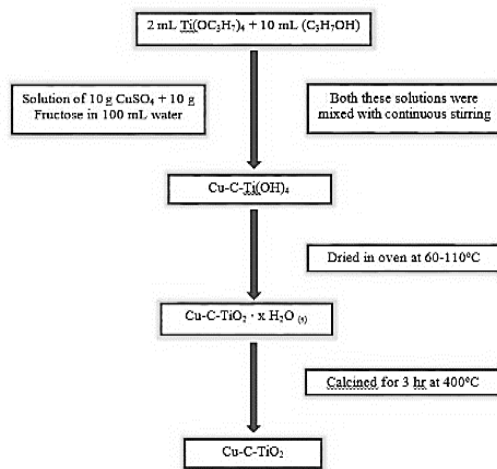


**Fig. 1.** Sol-gel method for the preparation of undoped and doped  $\text{TiO}_2$

## 2.2 Fabrication of Cell

The photoanode was prepared with Cu-C- $\text{TiO}_2$  paste in acetic acid with few drops of dishwashing liquid as a surfactant. This paste was coated onto the FTO glasses (2.2 mm thickness, 7-9 ohms  $\text{cm}^{-2}$ , L 25 mm x W 25 mm, Shilpa Enterprises, Nagpur, India) by doctor blade method and left for a few minutes to let it dry. Then the glass was heated on a hot plate at 450°C for 45 minutes. A solution of rhodamine B ( $1.0 \times 10^{-3}$  M) dye in ethanol was used for the sensitization of the working electrode. The working electrode was immersed in dye solution for 15 minutes and then rinsed with ethanol to remove extra dye. A graphite coated counter electrode was clipped onto the top of the working electrode. 0.43 M iodine and 0.46 M potassium iodide was dissolved in 10 mL of ethylene glycol. This  $\text{I}^-/\text{I}_3^-$  redox shuttle was used as liquid electrolyte.

## 3. Characterization of doped Cu-C- $\text{TiO}_2$ and undoped $\text{TiO}_2$

### 3.1 FTIR spectra of doped Cu-C- $\text{TiO}_2$

The Fourier Transform Infrared Spectroscopy (FTIR) spectra of the synthesized samples in potassium bromide (KBr) pellets were recorded on a Perkin Elmer Spectrum RX1 spectrometer in the range from 4400  $\text{cm}^{-1}$  to 450  $\text{cm}^{-1}$  at a scanning rate of 1  $\text{cm}^{-1}/\text{min}$ . The FTIR spectra of Cu-C- $\text{TiO}_2$  is given in Fig. 2. The peaks between 1620-1630  $\text{cm}^{-1}$  and the broad peaks appearing in between 3100-3600  $\text{cm}^{-1}$  are assigned as vibrations of hydroxyl groups [13]. The broad peaks at 3483  $\text{cm}^{-1}$  and the peaks at 1623  $\text{cm}^{-1}$  are characteristic of the H-O bending mode of hydroxyl groups present on the surface due to moisture. These are crucial to the photocatalytic reactions, since they can react with photoexcited holes generated on the catalyst surface and produce hydroxyl radicals [14]. Twin peaks at 639 and 617  $\text{cm}^{-1}$  indicated the Cu-O stretching vibration. The metal salt (Cu-O-C) peak is appeared at 1150  $\text{cm}^{-1}$  [15]. The vibrational mode of  $\nu$  Ti-O-Ti appeared at 488  $\text{cm}^{-1}$  [16] while Cu-O bending was observed at 520  $\text{cm}^{-1}$  [17]. The bands appearing at 520-590  $\text{cm}^{-1}$  are due to stretching vibrations of M-O (Ti-O & Cu-O). The band at 1111  $\text{cm}^{-1}$  is assigned to the  $\nu$ (Ti-O-C) bridging vibrations of isopropoxy groups [18, 19]. The peak at 852  $\text{cm}^{-1}$  is related to the

isopropoxide group. The peak present at 988  $\text{cm}^{-1}$  is due to antisymmetric stretching of Ti-O bonds in Ti-O-Ti [20-22].

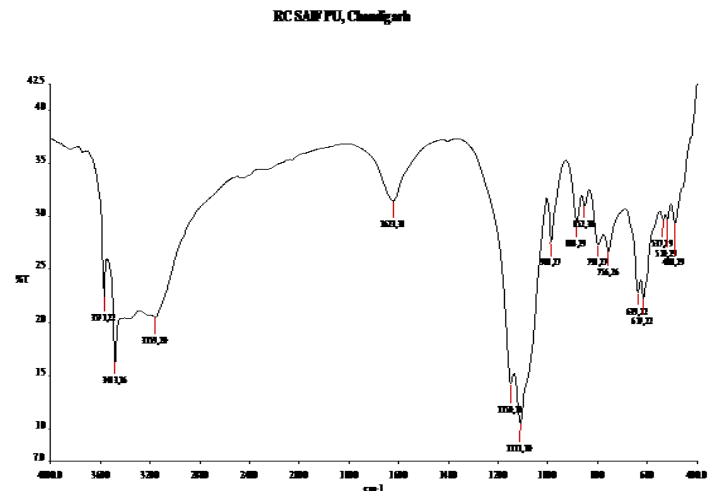


**Fig. 2.** FTIR spectra of Cu-C- $\text{TiO}_2$

### 3.2 X-ray Diffraction

The average crystalline size (D) of the undoped and Cu-C- $\text{TiO}_2$  material can be calculated from the Debye-Scherrer formula.

$$D = \frac{K\lambda}{\beta \cos \theta} \quad \text{---(1)}$$

Where D is the crystalline size (nm),  $\lambda$  is the wavelength (nm),  $\beta$  is the full width at half maximum intensity (FWHM-in radian), and  $\theta$  is the Bragg diffraction angle ( $^\circ$ ). The X-ray diffraction of undoped  $\text{TiO}_2$  and Cu-C- $\text{TiO}_2$  samples are given in fig. 3 and 4. The XRD patterns were recorded on Panalytical X'pert Pro model X-ray diffraction using Cu K $\alpha$  radiation as the X-ray source. The diffractograms were recorded in the  $2\theta$  range of 20-80 $^\circ$ . It is also confirmed by the spectra that both undoped and doped  $\text{TiO}_2$  are crystalline in nature. The average crystalline size of the undoped  $\text{TiO}_2$  is 10.15 nm and Cu-C- $\text{TiO}_2$  is 70.87 nm. However, it was observed that after doping the particle size is increases.

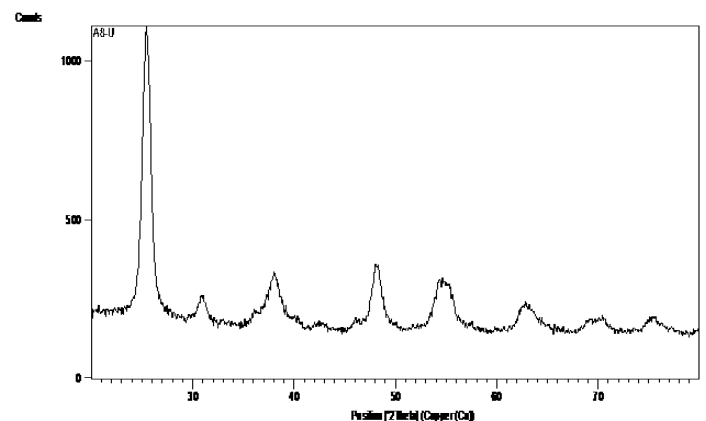


**Fig. 3.** XRD of undoped  $\text{TiO}_2$

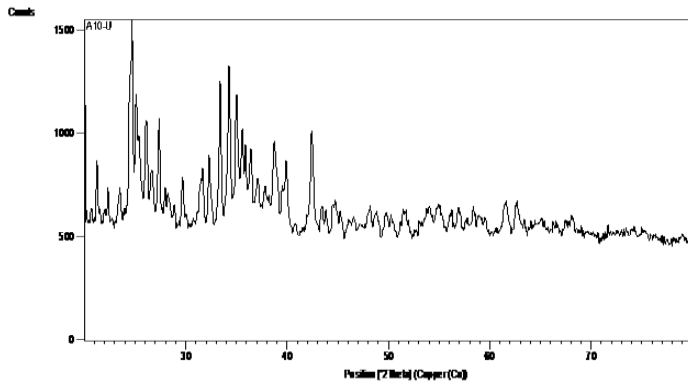


Fig. 4. XRD of Cu-C-TiO<sub>2</sub>

**3.3 Scanning Electron Microscopy (SEM)**

The morphology of undoped (Fig. 5a) and doped TiO<sub>2</sub> (Fig. 5b) was studied. SEM has been used to observe the morphological changes caused by loading of metal and non-metal on the surface of titania. It observed that incorporation of the dopants Cu and Carbon on TiO<sub>2</sub> increases particle size (From XRD data).

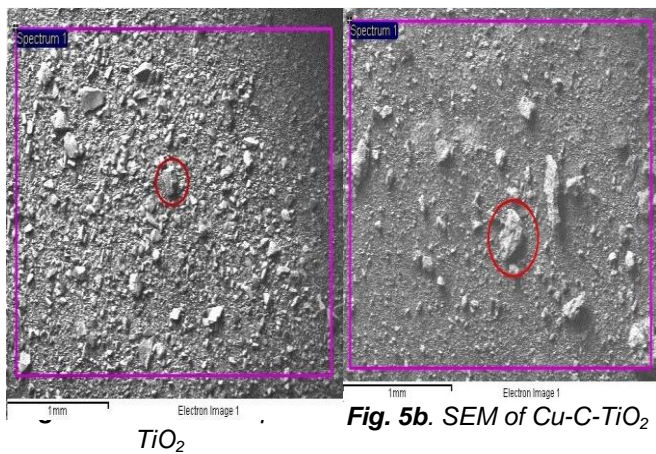


Fig. 5b. SEM of Cu-C-TiO<sub>2</sub>

**4. PHOTOVOLTAIC PERFORMANCE OF DSSC**

**4.1 Variation of potential with time**

The effect of variation of potential with time on the electrical output of the cell was observed, and results are reported in Table 1. The cell was placed in dark and the potential was measured. Then, the cell was exposed to light (66.0 mWcm<sup>-2</sup>). A change in potential was observed with the time of illumination. The potential was measured with digital multimeter (Mastech-M830bZ). The cell was charged for 70 minutes, as it attained a constant potential. Then the irradiation was cut off. It was observed that the potential starts increasing with time, but it never reached its initial value indicating that the reaction is not completely reversible.

Table 1. Variation of potential with time

| Time (min.) | Potential (mV) | Time (min.) | Potential (mV) |
|-------------|----------------|-------------|----------------|
| 0.0         | -194.5         | 75          | -24.8          |
| 5           | -96.6          | 80          | -28.8          |

|                |       |     |       |
|----------------|-------|-----|-------|
| 10             | -51.7 | 85  | -28.9 |
| 15             | -41.8 | 90  | -28.5 |
| 20             | -31.4 | 95  | -27.8 |
| 25             | -25.9 | 100 | -27.1 |
| 30             | -22.5 | 105 | -26.8 |
| 35             | -20.7 | 110 | -26.5 |
| 40             | -20.5 | 115 | -26.3 |
| 45             | -20.1 | 120 | -26.1 |
| 50             | -20.1 | 125 | -25.9 |
| 55             | -20.0 | 130 | -25.8 |
| 60             | -20.0 | 135 | -25.7 |
| 65             | -20.0 | 140 | -25.8 |
| 70 (light off) | -20.7 |     |       |

[Rhodamine B] = 1.3 x 10<sup>-3</sup> M; Electrolyte = [I<sub>2</sub>] = 0.43 M [KI] = 0.46 M; Exposed surface area = 1.3 x 1.3 cm<sup>2</sup>; LightIntensity = 66.0 mWcm<sup>-2</sup>

**4.2 Variation of Current with time**

The effect of variation of Current with time on the electrical output of the cell was observed, and results are reported in Table 2. The current was measured with a digital multimeter (Mastech-M830bZ). The photocurrent of cell rapidly increases on illumination and after a few minutes, it reaches to its maximum. This current is represented as *i<sub>max</sub>*. When illumination time was further increased, the current starts decreasing gradually, and it reaches an equilibrium value. This value is represented as *i<sub>eq</sub>*. When the source of illumination was removed, the current starts decreasing further.

Table 2. Variation of current with time

| Time (min.)    | Photocurrent (µA)              | Time (min.) | Photocurrent (µA) |
|----------------|--------------------------------|-------------|-------------------|
| 0.0            | 3.8                            | 75          | 8.5               |
| 5              | 54.4                           | 80          | 5.4               |
|                | ( <i>i<sub>max</sub></i> )     |             |                   |
| 10             | 34.1                           | 85          | 4.4               |
| 15             | 27.0                           | 90          | 3.7               |
| 20             | 19.9                           | 95          | 3.7               |
| 25             | 16.0                           | 100         | 2.9               |
| 30             | 13.8                           | 105         | 3.0               |
| 35             | 12.6                           | 110         | 3.3               |
| 40             | 11.6                           | 115         | 2.6               |
| 45             | 11.6                           | 120         | 2.3               |
| 50             | 11.6                           | 125         | 2.2               |
| 55             | 11.5                           | 130         | 2.1               |
| 60             | 11.4                           | 135         | 2.0               |
| 65             | 11.3                           | 140         | 2.0               |
| 70 (Light off) | 11.5 ( <i>i<sub>eq</sub></i> ) |             |                   |

[Rhodamine B] = 1.3 x 10<sup>-3</sup> M; Electrolyte = [I<sub>2</sub>] = 0.43 M [KI] = 0.46 M; Exposed surface area = 1.3 x 1.3 cm<sup>2</sup>; Light intensity = 66 mWcm<sup>-2</sup>

**4.3 Effect of dye concentration**

The dependence of the photopotential and the photocurrent on the dye concentration was observed by taking different concentration of rhodamine B (1.6 x 10<sup>-3</sup> M – 3.0 x 10<sup>-4</sup> M), and the results are reported in Table 3. It was observed that the electrical output of the cell increased on increasing the

concentration of rhodamine B. Thereafter it shows a reverse trend on increasing concentration of dye further. It may be explained of the bases that as the concentration of dye was increased, the number of sensitizer molecules also increases resulting in higher output of the cell. A reverse trend was observed on increasing of concentration of dye further. It may be due to the effect that dye starts acting as internal filter for the incident light and does not permit the desired intensity of the light to reach to semiconducting photoanode.

**Table 3. Effect of dye concentration**

| [Dye]<br>( $10^3$ M) | Potential (mA) | Current ( $\mu$ A) |
|----------------------|----------------|--------------------|
| 1.6                  | 68.35          | 21.2               |
| 1.3                  | 101.2          | 54.5               |
| 1.0                  | 126.4          | 32.4               |
| 0.6                  | 118.9          | 35.9               |
| 0.3                  | 79.9           | 7.9                |

Exposed surface area =  $1.3 \times 1.3 \text{ cm}^2$ ; Electrolyte =  $[I_2] = 0.43 \text{ M}$  [KI] =  $0.46 \text{ M}$ ; Light intensity =  $66.0 \text{ mWcm}^{-2}$

#### 4.4 Effect of electrolyte concentration

The effect of concentration of the component of liquid electrolyte ( $I_2$  and KI) on the electrical power of the cell was observed, and the results are reported in the Tables 4 and 5. For this purpose the concentration of one component was kept constant while other was varied. It was observed that as the concentration of iodine was increased, the potential and current both decrease, while on increasing the concentration of potassium iodide, there was a decreasing behavior in potential but increasing in current. The optimum conditions were obtained for  $I_2$  as  $0.43 \text{ M}$  and KI as  $0.46 \text{ M}$ .

**Table 4. Effect of concentration of iodine**

| $[I_2]$<br>(M) | Potential (mA) | Current ( $\mu$ A) |
|----------------|----------------|--------------------|
| 0.39           | 91.0           | 23.4               |
| 0.43           | 101.2          | 54.3               |
| 0.47           | 53.0           | 48.5               |
| 0.51           | 40.6           | 46.1               |
| 0.55           | 33.8           | 35.9               |

[Rhodamine B] =  $1.3 \times 10^{-3} \text{ M}$ ; Exposed surface area =  $1.3 \times 1.3 \text{ cm}^2$ ; Light intensity =  $66.0 \text{ mWcm}^{-2}$

**Table 5. Effect of concentration of potassium iodide**

| KI<br>(M) | Potential (mA) | Current<br>( $\mu$ A) |
|-----------|----------------|-----------------------|
| 0.44      | 74.2           | 2.5                   |
| 0.46      | 101.2          | 54.3                  |
| 0.48      | 56.7           | 28.5                  |
| 0.50      | 37.0           | 20.4                  |
| 0.51      | 21.0           | 16.6                  |

[Rhodamine B] =  $1.3 \times 10^{-3} \text{ M}$ ; Exposed surface area =  $1.3 \times 1.3 \text{ cm}^2$ ; Light Intensity =  $66.0 \text{ mWcm}^{-2}$

#### 4.5 Effect of exposed surface area of electrode

The effect of surface area of semiconductor was also observed, and the results are reported in Table 6. The potential and current increase with increasing area of electrode. It may be due to more exposed area of electrode.

**Table 6. Variation in exposed surface area**

| Area ( $\text{cm}^2$ ) | Potential (mA) | Current ( $\mu$ A) |
|------------------------|----------------|--------------------|
| $1.3 \times 1.3$       | 101.2          | 54.5               |
| $1.1 \times 1.1$       | 80.2           | 41.6               |
| $1.0 \times 1.0$       | 75.4           | 32.8               |
| $0.8 \times 0.8$       | 50.1           | 20.4               |
| $0.6 \times 0.6$       | 43.8           | 5.8                |

Rhodamine B =  $1.3 \times 10^{-3} \text{ M}$ ; Electrolyte =  $[I_2] = 0.43 \text{ M}$  and [KI] =  $0.46 \text{ M}$ ; Light Intensity =  $66 \text{ mWcm}^{-2}$

#### 4.6 Effect of light intensity

The effect of light intensity on electrical output of cell was observed, and the results are reported in Table 7. Light intensity may also affect the electrical parameters of DSSC and therefore light intensity was changed from  $50.0$  to  $66.0 \text{ mWcm}^{-2}$ . It shows an increasing trend with increasing light intensity because an increase light intensity increases the photons per unit area.

**Table 7. Variation of light intensity**

| Light Intensity<br>( $\text{mWcm}^2$ ) | Potential (mA) | Current ( $\mu$ A) |
|--|----------------|--------------------|
| 30.0                                   | 64.5           | 20.4               |
| 40.0                                   | 71.3           | 23.0               |
| 50.0                                   | 80.2           | 29.2               |
| 60.0                                   | 93.0           | 33.8               |
| 66.0                                   | 101.2          | 54.5               |

[Rhodamine B] =  $1.3 \times 10^{-3} \text{ M}$ ; Electrolyte =  $[I_2] = 0.43 \text{ M}$  and [KI] =  $0.46 \text{ M}$ ; Exposed surface area =  $1.3 \times 1.3 \text{ cm}^2$

#### 4. i<sub>5</sub>. i-V CHARACTERISTICS OF THE CELL

The open circuit voltage ( $V_{oc}$ ) (keeping the circuit open) and short circuit current ( $i_{sc}$ ) (keeping the circuit closed) of the cell were measured with a digital multimeter. The values of photocurrent and photopotential were observed with the help of a carbon pot (log 470 k) connected in the circuit by applying an external load. The variation of potential with respect to current is presented in Table 8 and graphically in Fig. 6.

**Table 8. i-V Characteristics**

| Potential (mV) | Photocurrent ( $\mu$ A) | Fill Factor |
|----------------|-------------------------|-------------|
| 101.2          | 0.0                     |             |
| 99.1           | 0.2                     |             |
| 92.8           | 2.6                     |             |
| 91.8           | 5.0                     |             |
| 89.6           | 9.6                     |             |

|      |      |      |
|------|------|------|
| 75.7 | 15.3 |      |
| 70.5 | 33.0 |      |
| 68.3 | 37.0 |      |
| 67.6 | 39.9 |      |
| 66.6 | 40.5 |      |
| 55.9 | 49.6 | 0.50 |
| 32.4 | 50.0 |      |
| 10.5 | 52.4 |      |
| 5.9  | 52.7 |      |
| 0.9  | 53.2 |      |
| 0.0  | 54.5 |      |

Rhodamine B =  $1.3 \times 10^{-3}$  M; Electrolyte =  $[I_2] = 0.43$  M and  $[KI] = 0.46$  M; Exposed surface area =  $1.3 \times 1.3 \text{ cm}^2$ ; Light Intensity =  $66 \text{ mWcm}^{-2}$

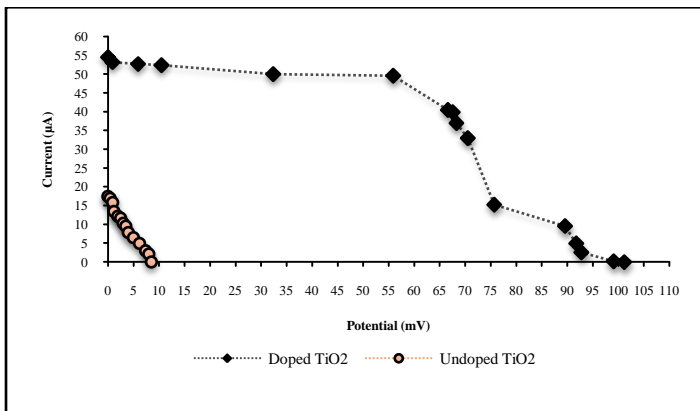


**Fig. 6.** The Photocurrent-voltage curve of doped and undoped  $TiO_2$  based DSSC

Values of  $V_{oc}$ ,  $V_{pp}$ ,  $i_{sc}$ , (voltage at power point) and  $i_{pp}$  (current at power point) were determined with the help of this curve. The maximum voltage at open circuit ( $V_{oc}$ ) was 101.2 mV where as the maximum current at short circuit ( $i_{sc}$ ) was 0.0545 mA. The 55.9 mV voltage ( $V_{pp}$ ) and 0.0496 mA current ( $i_{pp}$ ) were obtained at power point. Using these values, the fill factor (FF) was calculated from equation (1). The fill factor was observed as 0.50.

$$\text{Fill Factor} = \frac{V_{pp} \times i_{pp}}{V_{oc} \times i_{sc}} \quad \text{---(2)}$$

## 5. CELL EFFICIENCY

The conversion efficiency of the cell is the ratio of electrical output at power point and the power of incident radiations. The solar energy-to-electricity conversion efficiency ( $\eta$ ) was determined by the equation (2). Where  $P_{in}$  is intensity of the incident light.

$$\eta = \frac{FF \times i_{sc} \times V_{oc}}{P_{in}} \times 100 \% \quad \text{---(3)}$$

The performance of cell was also calculated using this relation. The cell showed 0.004 % over all power conversion efficiency. Comparative electrical parameters, fill factor, and conversion efficiency of DSSC with undoped and co-doped  $TiO_2$  are given in Table 9.

**Table 9.** Comparative results with undoped and co-doped  $TiO_2$  in DSSC.

| Sample        | $i_{pp}$ (mA) | $V_{pp}$ (mV) | $i_{sc}$ (mA) | $V_{oc}$ (mV) | FF  | $\eta \times 10^2$ (%) |
|---------------|---------------|---------------|---------------|---------------|-----|------------------------|
| Pure $TiO_2$  | 0.003         | 9.6           | 0.008         | 17.5          | 0.2 | 0.00654                |
| Cu-C- $TiO_2$ | 0.049         | 55.9          | 0.054         | 101.2         | 0.5 | 0.4                    |

## 6. PERFORMANCE OF CELL

The performance of cell was measured by applying the external load necessary to have current and potential at power point, after removing the source of illumination. It is the time taken in decreasing half of its maximum power. It was observed that the electrical output does not reach zero even after 70 minutes. The cell worked for 10 minutes even in the dark.

## 7. CONCLUSIONS

Co-doped semiconductor (Cu-C- $TiO_2$ ) was synthesized with sol-gel method. A DSSC was assembled with this semiconductor. A mixture of  $I_2$  and KI was used as electrolyte. The observation showed that doping of metal and non-metal increased the photocatalytic activity of semiconductor in visible light. The performance of cell was improved, when compared with undoped  $TiO_2$ . The cell fabricated with doped material was 61.11 time more efficient than undoped material.

## 8. ACKNOWLEDGMENT

Thanks are due to head department of chemistry PAHER University for providing necessary laboratory facilities. We are also thankful to director, SAFI Panjab University Chandigarh for providing FT-IR and XRD data and M S Vadodara University, Gujrat for SEM data.

## REFERENCES

- [1] T.M.Razykov, C.S.Ferekides, D.More, E.Stefanakos, H.S.Ullal, H.M.Upadhyaya, "Solar Photovoltaic Electricity: Current Status and Future Prospects", *Solar Energy*, vol. 85, no. 8, pp.1580–1608, Aug.2011, doi:10.1016/j.solener.2010.12.002.
- [2] B.O'Regan and M. Gratzel, "A Low-Cost, High-Efficiency Solar Cell Based on Dye-Sensitized Colloidal  $TiO_2$  Films", *Nature*, vol. 353, no. 24, pp. 737-740, Oct.1991, doi:10.1038/353737a0.
- [3] A.Hagfeldt, "Brief Overview of Dye-Sensitized Solar Cells", *Ambio*, vol. 41, pp. 151-155, Mar. 2012. doi: 10.1007/s13280-012-0272-7

- [4] S.Mathew, A.Yella, P.Gao,R.Humphry-Baker, B.F.E.Curchod, N. Ashari-Astani,I.Tavernelli,U.Rothlisberger,Md. K.Nazeeruddin and M. Grätzel, "Dye-Sensitized Solar Cells With 13% Efficiency Achieved Through The Molecular Engineering of Porphyrin Sensitizers", *Nature Chemistry*, vol. 6, pp. 242–247, Feb. 2014,doi:10.1038/nchem.1861.
- [5] M.H. Kim, and Y.U. Kwon, "Semiconductor CdO as a blocking layer material on DSSC electrode: Mechanism and application", *The Journal of Physical Chemistry C*, vol. 113, no. 39. pp. 17176–17182, Sep. 2009, doi:10.1021/jp904206a.
- [6] M. Kaur, and N.K. Verma,"Structural and optical properties of  $\text{Eu}_2\text{O}_3$  coated  $\text{TiO}_2$  nanoparticles and their application for dye sensitized solar cell", *Journal of Materials Science: Materials in Electronics*, vol. 24, no.4, pp.1121-1127, Apr. 2013,doi: 10.1007/s10854-012-0892-5.
- [7] Z. Li, D. Ding, Q.Liu, and C. Ning, "Hydrogen sensing with Ni-doped  $\text{TiO}_2$  nanotubes", *Sensors*,vol. 13, no. 7, pp. 8393-8402.Jun. 2013,doi:10.3390/s130708393.
- [8] J.Y.Park, K.H.Lee, B.S.Kim, C.S.Kim, S.E.Lee, K. Okuyama, H.D.Jang, and T.O.Kim, "Enhancement of dye-sensitized solar cells using Zr/N-doped  $\text{TiO}_2$  composites as photoelectrodes", *RSC Advance*, vol. 4, pp. 9946-9952. Feb. 2014,doi:10.1039/C4RA00194J.
- [9] F.Gu, W.Huang, S.Wang, X.Cheng, Y.Hu, and P.S.Lee, "Open-circuit voltage improvement in tantalum-doped  $\text{TiO}_2$  nanocrystals" *Physical Chemistry Chemical Physics*,vol. 16, no. 47, pp. 25679-2568, Dec. 2014,doi: 10.1039/C4CP01655F.
- [10] T.Ma, M.Akiyama, E.Abe, and I. Imai,"High-efficiency dye-sensitized solar cell based on a nitrogen-doped nanostructured titania electrode", *Nano Letters*, vol. 5, no. 12, pp. 2543–2547,Nov. 2005, doi: 10.1021/nl051885l.
- [11] G.Xie, Y.Weil, L.Fan, and J. Wu, "Application of doped rare-earth oxide  $\text{TiO}_2\text{:}(\text{Tm}^{3+}, \text{Yb}^{3+})$  in dye-sensitized solar cells", *Journal of Physics: Conference Series*, vol. 339, 012010, 2012,doi:10.1088/1742-6596/339/1/012010.
- [12] Y.Z.Zheng, J.X.Zhao, S.Q.Bi, X.Tao, M.Huang, J.F.Chen,"Dual interfacial modifications of hierarchically structured iodine-doped ZnO photoanodes for high-efficiency dye-sensitized solar cells", *Electrochimica Acta*, vol. 157, pp.258–265,Mar. 2015,doi:10.1016/j.electacta.2015.01.035.
- [13] K. Nakamoto, "Infrared and raman spectra of inorganic and coordination compounds", *John Wiley & Sons: New York*, 1986.
- [14] Z.Ding G.Q. Lu, and P.F.Greenfield, "Role of the crystallite phase of  $\text{TiO}_2$  in heterogeneous photocatalysis for phenol oxidation in water", *Journal of Physical Chemistry B*, vol. 104, no. 19, pp. 4815-4820, Apr. 2000,doi:10.1021/jp993819b.
- [15] H.H.Chen, R.Anbarasan, L.S.Kuo, M.Y.Tsai, P.H.Chen, and K.F.Chiang, "Synthesis, characterizations and hydrophobicity of micro/nano scaled heptadecafluorononanoic acid decorated copper nanoparticle", *Nano-Micro Letters*, vol. 2, no. 2, pp. 101-105, May 2010,doi: 10.5101/nml.v2i2.p101-105.
- [16] A.F.L.Almeida, D.R.S.Oliveira, J.C.Goes, J.M. Sasaki, A.G S. Filho, J.M.Filho, A.S.B Sombra, "Structural properties of  $\text{CaCu}_3\text{Ti}_4\text{O}_{12}$  obtained by mechanical alloying", *Materials Science and Engineering: B*, vol. 96, no. 3, pp.275-283, Dec. 2002, doi:10.1016/S0921-5107(02)00379-3.
- [17] X. S.Sahaya and C.Mahadevan,"FT-IR spectroscopic and thermal studies on pure and impurity added calcium tartrate tetrahydrate crystals", *Crystal Research and Technology*, vol. 40, no. 6, pp.598-602, Apr.2005, doi:10.1002/crat.200410389.
- [18] R.Urlaub, U.Posset, and R. Thull, "FT-IR spectroscopic investigations on sol-gel-derived coatings from acid modified titanium alkoxides", *Journal of Non-Crystalline Solids*,vol. 265, no. 3, pp. 276-284, Mar, 2000, doi:10.1016/S0022-3093(00)00003-X.
- [19] F.N.Castellano, J.M.Stipkala, L.A.Friedman and G.L Meyer, "Spectroscopic and excited-state properties of titanium-dioxide gels", *Chemistry of Materials*, vol. 6, no. 11, pp.2123-2129, Nov.1994, doi:10.1021/cm00047a037.
- [20] K. V.P.M. Shafi, A. Ulman, X. Yan, N.L. Yang, M. Himmelhaus, M. Grunze, "sonochemical preparation of silane-coated titania particles", *Langmuir*, vol. 17, no. 5, pp. 1726-1730, Feb. 2001, doi: 10.1021/la001252g.
- [21] H.Lee and W.C.Chen, "High-refractive-index thin films prepared from trialkoxysilane-capped poly(methyl methacrylate)-titania materials", *Chemistry Materials*, vol. 13, no. 3, pp.1137-1142, Feb. 2001,doi: 10.1021/cm000937z.
- [22] R. Nakamura, A. Imanishi, K.Murakoshi, and Y.Nakato, "In situ FTIR studies of primary intermediates of photocatalytic reactions on nanocrystalline  $\text{TiO}_2$  films in contact with aqueous solutions", *Journal of American Chemistry Society*, vol. 125, no. 24, pp. 7443-7450, May 2003,doi:10.1021/ja029503q.